



Lateral torsional buckling and torsional bracing of steel girder systems

Todd Helwig¹

Abstract

This paper accompanies the 2025 Beedle Lecture and outlines work conducted over the past 30+ years that the author had the privilege to work on along with a group of outstanding graduate students, post-doctoral researchers, and colleagues. The studies focus on a variety of problems related to buckling and bracing of members and structural systems. The topic of this paper is primarily directed specifically on lateral-torsional buckling investigations along with torsional beam bracing. The understanding of the fundamental buckling and bracing behavior have improved dramatically since the early 1990's and this paper summarizes some of the advances. The studies on lateral torsional buckling are focused on the effects of moment gradient, solutions for non-prismatic members, as well as system-buckling of girder systems. The torsional beam bracing studies included several factors that impact both the stiffness and strength requirements for the bracing. An overview of several of these studies is provided along with a discussion of provisions that have been incorporated into design specifications for buildings and bridges in the United States.

1. Introduction

The limit state of lateral torsional buckling (LTB) often controls the design of I-shaped girders. The buckling strength is improved with the use of bracing to reduce the unbraced length of the girders. While there are a number of stages for which LTB may control, the construction stage is often critical, particularly for girders that are designed to act composite with a concrete slab/deck during in-service conditions. During construction, freshly-placed concrete is fluid and provides no significant contribution towards the buckling resistance of the girders. Therefore, the steel girder is generally designed to support the entire construction load during the concrete placement. Another complexity that exists during construction is the variable presence of the bracing, since not all of the bracing is usually fully installed during girder erection.

Effective beam bracing can be achieved by preventing either lateral movement of the compression flange (lateral bracing) or twist of the girder cross-section (torsional bracing). The primary bracing that is discussed in this paper is torsional bracing that often exists in the form of cross-frames or diaphragms that frame into the girders at isolated points along the length.

This paper outlines a number of studies that have been conducted over the past 30+ years that are focused on LTB of steel beams and girders as well as the torsional-bracing behavior to improve the buckling strength. The paper begins with pertinent background information on both LTB and bracing, followed by an overview of some of the research related to LTB and torsional bracing that have impacted US design specifications in the past few decades.

¹ Jewel McAlister Smith Professorship in Engineering, University of Texas at Austin , <thelwig@mail.utexas.edu>

2. Background

2.1 Lateral Torsional Buckling

Lateral torsional buckling (LTB) is a limit state for beams and girders that generally involves a lateral translation of the compression flange and a twist of the girder cross section. Timoshenko (1961) derived the classic equation for elastic LTB of a doubly-symmetric section subjected to uniform moment loading that is given by the following expression:

$$M_o = \frac{\pi}{L_b} \sqrt{EI_y GJ + \left(\frac{\pi EI_y h_o}{2L_b}\right)^2} \quad (1)$$

where, E is the modulus of elasticity, I_y is the minor-axis moment of inertia of the girder about the plane of the web, L_b is the unbraced length, G is the shear modulus of elasticity, J is the torsional constant, and h_o is the distance between flange centroids. In addition to uniform moment along the unbraced length, Eq. (1) was derived also assuming that the member was free to warp at the ends. The equation is often given with the 2nd term in the radical expressed as a function of the warping constant for a doubly symmetric I-shaped member, $C_w = I_y h_o^2 / 4$.

Although Timoshenko's solution was derived for uniform moment loading, in practice most beams are subjected to moment gradient that leads to a variable flange compressive stress along the length. The benefits of variable moment are usually accounted for with a moment gradient factor (C_b) applied to the uniform moment expression. There are a variety of moment gradient factors that are available for specific loading distributions and support conditions. For a doubly-symmetric beam buckling between discrete brace points, the AISC Specification (2022) recommends the following expression:

$$C_b = \left[\frac{12.5M_{max}}{2.5M_{max} + 3M_A + 4M_b + 3M_C} \right] \quad (2)$$

where, M_{max} is the absolute value of the maximum moment in the unbraced segment, M_A , M_b , M_C are the respective absolute values of the quarter-point, midpoint, and three-quarter-point moment in the unbraced segment. Equation (2) is just one expression that can be used to estimate the moment gradient factor. There are a number of other expressions available in the literature (SSRC, 2010) that are applicable for a variety of conditions. Many C_b equations are developed for loads applied at midheight of the section. Load position effects occur when the load is applied at locations above or below midheight. Considering gravity loading, relative to midheight loading, loads applied higher on the cross-section are detrimental, while loads applied lower on the section are beneficial. Recommendations are available in the literature (SSRC 2010) that modify the moment gradient factors to account for load position.

While Eq. (1) provides a solution for doubly-symmetric sections, the buckling behavior of singly-symmetric I-shaped sections is more complex and the exact elastic solution (Galambos 1968, SSRC 2010) recognizes the increased complexity. While the exact solution is useful for research applications, in design most specifications (AISC 2022, AASHTO (2024) make use a simplified LTB solution that is within approximately 10% of the exact solution for most singly-symmetric I-sections unless one of the flanges becomes very small and the section approaches a T-shaped section.

2.2 Stability Bracing

The pioneering work of Winter (1960) demonstrated the dual criteria for effective stability bracing that includes both stiffness and strength requirements. Winter's work focused heavily on lateral bracing of columns that was extended to flexural members. Winter developed a simple model that allowed the determination of the "ideal stiffness" requirements to be established for lateral bracing in columns and beams. The ideal stiffness can be generally defined as the minimum stiffness necessary to cause a perfectly straight member to buckle between the brace points. Winter also demonstrated the impact of imperfections on the brace forces and further established that a stiffness higher than the ideal stiffness was necessary to control brace forces and deformation in the member. For most problems, doubling the ideal stiffness requirements results in a maximum deformation at the design load that is equal to the magnitude of the initial imperfection and the brace force is therefore essentially equal to the brace stiffness multiplied by the magnitude of the initial imperfection.

Taylor and Ojalvo (1966) produced solutions for torsional bracing of beams considering continuously-braced members. Perhaps the most influential work related to bracing of beams was conducted by Yura (2001) that built off of the previous work and considered many of the fundamental factors that impact bracing systems. The work from Yura considered many factors such as moment gradient, load position, and the impact of cross-sectional distortion on the effectiveness of bracing. For torsional-braced beams, a reasonable estimate of the ideal stiffness of a bracing system can be represented with the following expression:

$$\beta_{Ti} = \frac{1.2L}{nEI_{yeff}} \left(\frac{M_r}{C_b} \right)^2 \quad (3)$$

where, L is the span of the beam, n is the number of intermediate brace points, I_{yeff} is the effective minor-axis moment of inertia, and M_r is the design moment within the unbraced length. For singly-symmetric sections, $I_{yeff} = I_{yc} + (t/c) I_{yt}$, where I_{yc} and I_{yt} are the moment of inertia of the respective compression and tension flanges about an axis through the web, while c and t are respective distances from the centroid of the section to the extreme fibers of compression and tension flanges. For doubly-symmetric sections, the effective moment of inertia is equal to the minor-axis moment of inertia of the section.

Beam torsional bracing is a function of multiple stiffness components with the most dominant components being i) the stiffness of the brace (β_b), ii) the in-plane stiffness of the girder (β_g), and the effect of cross-sectional distortion (β_{sec}). Similar to many stability bracing systems, the total stiffness of the bracing system (β_T) is governed by the expression for springs in series:

$$\frac{1}{\beta_T} = \frac{1}{\beta_b} + \frac{1}{\beta_{sec}} + \frac{1}{\beta_g} \quad (4)$$

Eq. (4) for springs in series mathematically dictates that the total brace stiffness of the system (β_T) will be less than the smallest stiffness component.

3. Studies on Beam Stability

3.1 Moment Gradient, Load Position, Buckling of Non-Prismatic Beams, and System Buckling Mode

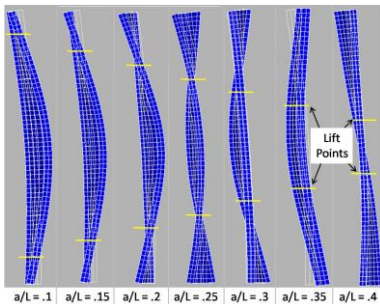
There have been a number of previous investigations on the LTB behavior of doubly-, singly- and un-symmetric flexural members. The critical stages often occur during erection and construction when both bracing and loading conditions are often the most unpredictable. In the completed structure, all of the bracing is present and additional restraint often develops from sources such as the cured concrete deck or even components that are not necessarily relied upon for stability. Restraints also often develop from phenomenon that is not directly relied upon in design since it may be hard to fully quantify. For example, beams often experience “tipping restraint” when loads are applied through structural members or non-composite slab systems; however, such restraint is difficult to quantify. However, these restraints may be recognized to help and might allow detrimental effects such as top-flange loading to be neglected during design. The following subsections provide brief overviews of studies that have been conducted related to LTB over the past several years.

3.1.1 LTB of Girders During Lifting

As noted earlier, erection and construction stages are often critical for stability due to the limited presence of bracing. One particular stage where bracing may be non-existent is during lifting of girders when the girder segments only source of support are the lifting points from the girders as shown in Figure 1. Girder segments were instrumented in the storage yard of WW AFCO in San Angelo, Texas to monitor the behavior during lifting (Stith et al. 2010). Additional studies were conducted by instrumenting and monitoring girders in the field during erection and deck construction. Parametric FEA studies were conducted to evaluate the buckling behavior of the



(a) Girder lifting



(b) Buckled shape with varying lift point

Figure 1 Girder Stability During Lifting

girders as a function of the lifting location. The resistance of the girder against buckling comes from the weight of the girder which is positioned below the beam lifting clamps on the flange. However, there is no location where twist of the girder is fully restrained. Defining “ a ” as the distance from the end of the girder to the lifting point, if the girders are picked up with the lift points closer to the ends of the segment, the region between the pick points dominate the buckled shape. As the distance to the lifting point (larger a) is increased, the buckling mode changes and is dominated by the overhanging segment. The researchers originally focused on developing recommendations based upon buckling of the overhang versus buckling of the region between the lift points; however, this approach was relatively complicated. Instead, because the girders are not fully restrained from twist at any location along the length, the study recommended using the full length of the girder as the unbraced length (Farris, 2008, Schue 2008). Practical lengths of the girder segments can range from 20 ft. to spliced girders with lengths over 200 ft. depending on whether the girders are from building or bridge applications. As a result, the study considered both prismatic and non-prismatic sections. For

prismatic sections, the ideal location of lifting is generally at the quarter points of the girders; however, most of the lifts are conducted with a single crane and a spreader beam as shown in Figure 1. Since the erector does not usually have a spreader beam of optimal length to put lifting points at the quarter points, the lifting points vary relative to the segment length. The recommended C_b factor was therefore put in terms of the lift points relative to the total segment length as follows (Farris 2008):

$$\begin{aligned}
 C_b &= 2.0 \quad \text{for} \quad \frac{a}{L} \leq 0.225 \\
 C_b &= 6.0 \quad \text{for} \quad 0.225 < \frac{a}{L} < 0.30 \\
 C_b &= 4.0 \quad \text{for} \quad \frac{a}{L} \geq 0.3
 \end{aligned}
 \tag{5}$$

Where, L is the total length of the girder segment being lifted and a is the average distance from the end of the girder segment to the lift point (see Figure 1). There is obviously a practical limit to a/L values larger than 0.3, with “upper limits” of about 0.35 before girder yielding will control due to the very large overhang. For a prismatic segment, the overhang lengths (a) will be the same on both ends of the girder; however, for a nonprismatic section with unsymmetric distributions of the girder self-weight, the lift points will be different from the two ends of the section and the distances are then simply averaged. As noted above, the unbraced length to be evaluated with the uniform moment solution (such as Eq. 1) is taken as the total length of the segment. For non-prismatic sections, the uniform moment LTB solution should make use of the smallest section properties along the segment. The C_b expressions have been calibrated based upon these assumptions and provide good estimates of the girder buckling behavior.

3.1.2 LTB Non-prismatic Girders

Efficient use of steel in longer span girders often necessitate the use of stepped flanges along the girder length as a function of the moment demands in the girders. It is very common to have a flange transition creating a non-prismatic section within the unbraced length that complicates the evaluation of the LTB response. For longer-span applications, many girders do not have all of the bracing installed early in the erection stage and multiple flange transitions often occur along the unbraced length, which further complicates assessing the LTB behavior. Reichenbach et al. (2020) conducted parametric FEA studies on singly-symmetric non-prismatic girders to develop simple provisions for evaluating the LTB behavior of the girders. In addition to studying non-prismatic sections, the study refined previous work (Helwig et al. 1997) related to load position and moment gradient effects for singly-symmetric sections. The discussions below apply to gravity loading on composite singly-symmetric girders that generally have a smaller top flange compared to the bottom flange. The top flange is smaller since the neutral axis of the composite girder will generally lie at or near the top flange of the section once the concrete slab/deck cures. However, during construction, the entire load is generally supported by the steel girder and LTB often controls the design. Around interior supports the sections are often doubly-symmetric sections since the concrete deck is in tension and provides little contribution. Reichenbach et al. (2020) recommended the following moment gradient factor for singly-symmetric sections:

$$C_b = \left[\frac{12.5M_{max}}{2.5M_{max} + 3M_A + 4M_B + 3M_C} \right] R_m \leq 3.0 \quad (6)$$

$$R_m = \begin{cases} 0.5 + 2(\rho_{top,base})^2, & otherwise \\ 1.0, & if \begin{cases} single - curvature bending \\ -1/2 < M_{small}/M_{large} < 0; \text{ and } x_{inf} < 3L_b/8 \end{cases} \end{cases} \quad (7)$$

Where, R_m is a modifier on the moment gradient factor for singly-symmetric sections, $\rho_{top,base}$ is a factor referring to the properties of the smaller (base) flange along the unbraced length and is equal to $I_{y_{top}}/I_y$ which is a ratio of the minor-axis moment of inertia of the top flange over the moment of inertia of the entire section about the minor-axis through the web, M_{small} smaller moment at the end of the unbraced length and M_{large} is the moment at the other end of the unbraced length. The variable x_{inf} is for cases with reverse curvature bending and is the distance to the inflection point measured from the end of the unbraced length with the smaller end moment. All other terms are as described previously in the paper. For a prismatic singly-symmetric section, $\rho_{top,base}$ is equal to $I_{y_{top}}/I_y$. Equation 6 is identical to the expression proposed in Helwig et al. (1997) that has been in the AISC Chapter F Commentary for several years. Reichenbach et al. (2020) found the modification to the limits on R_m given in (7) provide better estimates when an inflection point is positioned very close to the end of the unbraced length with the smaller moment (ie, a very small length of the top flange is in compression). Eqs. (6) and (7) are included in Appendix D to the 10th ed. of AASHTO (2024).

Reichenbach et al. (2020) also develop recommendations on the evaluation of the LTB behavior for sections with multiple transitions in the width or thickness of flanges and webs along the length of the member. They recommended effective plate properties of the top and bottom flanges that are reflected in the following expressions:

$$b_{eff} = b_{small}[1 - (1 - x_{small})^2] + b_2(1 - x_{small})^2 \quad (8)$$

$$t_{eff} = t_{small}[1 - (1 - x_{small})^2] + t_2(1 - x_{small})^2 \quad (9)$$

where, b_{eff} and t_{eff} are the respective effective width and thickness of the flange under consideration with transitions along the unbraced length, b_{small} and t_{small} is the respective width and thickness of the segment with the smallest flange, b_2 and t_2 are the width and thickness of the 2nd smallest flange size along the unbraced length, and x_{small} is the decimal fraction of the length of the smallest flange section relative to the overall unbraced length. Each flange is treated separately and values of the effective widths and thickness are determined. An effective thickness can also be arrived at with Eq. (9) for variations in web thickness. For web-tapered members, a similar expression is proposed that differs slightly from Eqs. 8 and 9. Once the effective plate sizes are determined using Eqs. (8) and (9) the non-prismatic section is treated as an effective prismatic section to calculate the

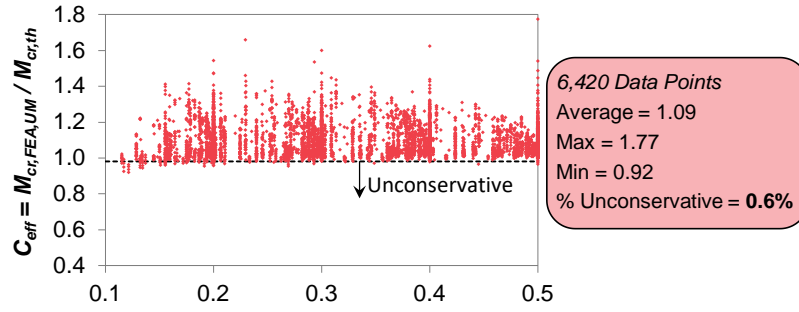


Figure 2: LTB Comparisons of FEA versus Predicted Solutions with Eff. Properties for Non-prismatic Sections with Uniform Moment.

coefficient $C_{eff} = M_{cr,FEA}/M_{cr,th}$ was evaluated, which is the ratio of the finite element eigenvalue buckling critical load to the calculated value using the exact analytical LTB expression with the effective section properties. Ratios less than 1 indicate the prediction is unconservative, while ratios greater than 1 indicate a conservative prediction. The results are summarized in Figure 2 for 6420 cases. The average accuracy is within 9% conservative of the FEA solutions.

3.1.3 Effect of Shear on LTB

Uniform moment buckling expressions such as Timoshenko's expression given in Eq. (1) are frequently used to evaluate the elastic buckling capacity of girders with compact and non-compact webs. For beams with slender webs, many design specifications make use of recommendations from Winter (1943) to account for web distortion by neglecting the St. Venant stiffness. This is the solution utilized in the AISC (2022) and AASHTO (2024) specifications leading to the following expression in terms of buckling stress:

$$F_{cr} = \frac{C_b \pi^2 E}{\left(\frac{L_b}{r_t}\right)^2} \quad (10)$$

$$r_t = \frac{b_{fc}}{\sqrt{12\left(1 + \frac{1}{6}a_w\right)}} \quad (11)$$

$$a_w = \frac{h_c t_w}{b_{fc} t_{fc}} \quad (12)$$

Where, b_{fc} and t_{fc} are the respective width and thickness of the compression flange, while h_c and t_w are the respective depth of the web in compression and web thickness. Yura recognized large discrepancies between classic LTB solutions such as Timoshenko's equation (with C_b factors) for beams subjected to significant moment gradient. The discrepancies were amplified with increasing web slenderness. Parametric FEA studies were carried out and reported in Liang et al. (2022, 2024) on both doubly- and singly-symmetric girders. The problem was identified to be related to the impact of shear that leads to distortional issues with the cross-section. The following solution was recommended:

$$M_{cr} = C_{mv} C_b M_o \quad (13)$$

section properties for use in the uniform moment buckling solution. Eqs. (8) and (9) are included in Appendix D6.6.3 of the AASHTO (2024) Bridge Design Specifications (BDS). Reichenbach et al. (2020) provide a comparison of the finite element solutions for non-prismatic sections with up to three flange transitions along the unbraced length with a wide variety of flange sizes. The

$$C_{mv} = \frac{V_{cr}}{V_{cr} + \alpha V_{st}} \quad (14)$$

Where, C_{mv} is a reduction factor accounting for the effects of shear on the LTB resistance, M_o is the uniform moment buckling capacity from expressions such as Eq. (1), C_b is the moment gradient factor for the specific loading and boundary conditions (there are lots of C_b expressions available), V_{cr} is the elastic shear buckling resistance, V_{st} is the shear magnitude that corresponds to a rigid web assumption and can be calculated from the following equation for a maximum design moment of M_{max} and an average shear along the unbraced length (V_{avg}):

$$V_{st} = V_{avg} \frac{C_b M_o}{M_{max}} \quad (15)$$

The value of α in Eq. 14 is related to the area of the web (A_w) and the average area of the flanges (A_f) as given in the following expression:

$$\alpha = 0.11 C_b \sqrt{A_w / A_f} \quad (16)$$

Whereas Winter's solution recommended neglecting the St. Venant term for beams with slender webs, the proposed method makes use of both the St. Venant and Warping terms in the LTB expression (M_o) regardless of the web slenderness. Comparisons between FEA solutions and the predicted solutions with the proposed solution (Eq. 13) and Winter's approach of neglecting the St. Venant terms are provided in Figure 3. The proposed solution provides good estimates of the effects of shear for a wide range of loading conditions. The results shown are for unstiffened webs; however, the behavior of stiffened webs was also considered with good agreement. The effects of web stiffeners are accounted for in the Liang et al. (2022, 2024) solution in the plate buckling coefficient in the elastic shear buckling capacity (V_{cr}). Winter's solution provided a simple approach for several decades to a relatively complicated problem. However, Figure 3 shows that Winter's solution can be significantly conservative or unconservative. Winter's solution tends to be conservative when the St. Venant stiffness was neglected for members with low shear relative to the shear buckling capacity and is unconservative for webs with large shear relative to the shear

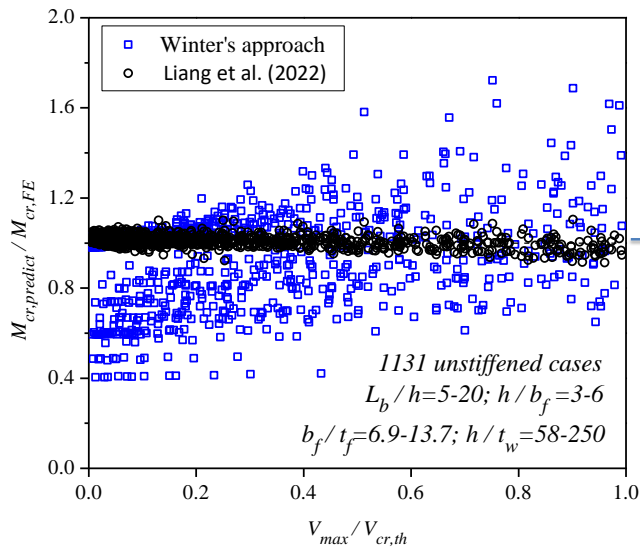
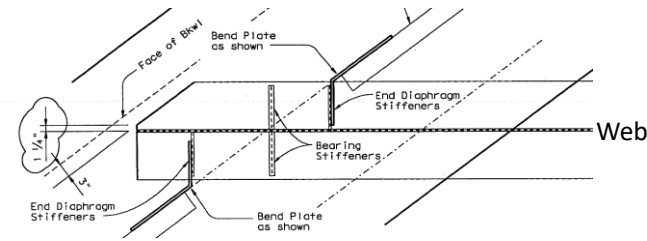


Figure 3: Effects of Shear on LTB Predictions from Liang et al. (2022) and Winter (1943)

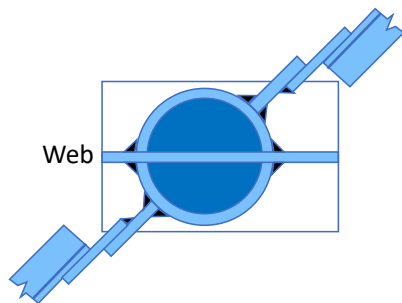
buckling capacity. Many of the cases that were unconservative had noncompact and even compact webs – but the high shear impacts the accuracy of the solution. In design, there are three options when the effects of shear are significant: 1) the web thickness can be increased resulting in an increase in the shear buckling capacity, 2) web stiffeners can be added resulting in an improved shear buckling coefficient and therefore an increased shear buckling capacity, or 3) bracing can be added to reduce the unbraced length and therefore improve the uniform moment buckling capacity, M_o . A numerical example is provided in Liang et al. (2022) demonstrating all three of these options.

3.1.4 Half-Round Bearing Stiffeners

Torsional bracing in the form of cross-frames or plate diaphragms are commonly used in steel bridges and sometime in steel buildings. In bridges with skewed supports, the AASHTO BDS (2022) require intermediate braces be oriented perpendicular to the girder lines for bridges with support skews larger than 20 degrees. For skew angles less than 20 degrees, the braces can be oriented parallel to the skew. However, at support regions, the braces are often parallel to the skew angle even for relatively large support skews. To facilitate the connections, many fabricators make use of bent plates such as that shown in Figure 4a which shows a plan view of the support region



a) Commonly-used detail with bent plate



b) Half-round bearing stiffener

Figure 4 Bent plate and half-round stiffener details for cross-frame connections

of a bridge with skewed supports. Pictures of the bent plate detail on a heavily skewed bridge are also shown later in Figure 14. The detail commonly makes use of a bearing stiffener directly over the support bearing as well as stiffeners that serve as cross-frame connection plates. A bent plate is commonly used for the connection between the connection plate stiffener and cross frame. The centerline of the brace passes directly over the support; however, the bent plate introduces significant flexibility into the connection. An alternative detail that provides perpendicular connections to the cross-frame connection plate consist of the half-round stiffener as shown in Figure 4b. The half-round can be made by either splitting a round pipe or bending a plate the proper radius. The half-round stiffener provides an excellent bearing stiffener due to the large buckling resistance as a column.

A major benefit to the half-round stiffener is that it can be welded to the web and both flanges creating a closed tube, which dramatically improves the warping stiffness at the stiffener. Ojalvo and Chambers (1977) provide a good discussion of the use of warping-restraining devices such as the half-round stiffener. A detailed investigation was conducted on the behavior of the bent plate versus the half-round stiffener with regards to girder stability as well as the fatigue performance of the welded connection and are documented in Quadrato et al (2010, 2014). The benefits of the warping restraint were demonstrated with both experiments and FEA parametric studies. The advantage of the use of plate stiffeners versus half-round stiffeners is shown in the experimental results for buckling tests on a W30x90 section. Figure 5 shows a comparison of the applied load versus the lateral deflection of the compression flange for girders with half-round bearing stiffeners versus plate stiffeners. The improved warping stiffness from the girder with the pipe stiffener increased the buckling resistance by approximately 50%. Quadrato et al. (2014) provides expressions for determining the effective length factor, K_w , that can be applied to the warping term in the buckling solution.

The AASHTO BDS (2022) now includes half-round stiffeners as an option for bearing stiffeners. While steel bridges tend to have longer spans, the structural advantages of the half-round stiffeners are likely to be in bridges with spans less than approximately 80 ft., which fit into geometries of the Short-Span Steel Bridge Alliance.

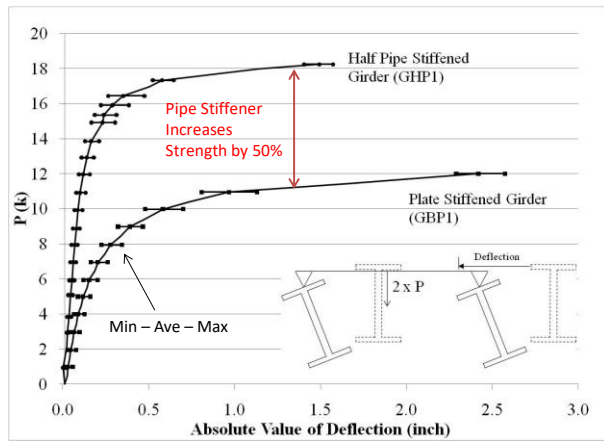


Figure 5: Improved Buckling Resistance with Half-Round Stiffeners versus Plate Stiffeners.

Experiments are currently being conducted at the University of West Virginia to assess the behavior for short span bridges. For the structural advantage with respect to buckling to be recognized, the half-round stiffener needs to be part of the critical unbraced segment of the girder. For a simply-supported girder, this would mean a maximum of a single intermediate brace. Brace spacing in conventional girders are often in the range of 20-30 ft. Due to the improved warping resistance, it is likely simple spans can be constructed with zero intermediate braces for spans up to approximately 40-50 ft. and up to 70-80 ft. with a single intermediate brace.

3.1.5 System Buckling Mode of Narrow Girder Units

Section 3.2 of this paper is focused on beam torsional bracing. Cross-frames and diaphragms are often provided to restrain twist of the cross-section. Although the 10th of the AASHTO BDS (2024) include torsional bracing requirements, historically, typical member sizes are often utilized in cross-frames to restrain the girders. Most bridge owners have specific details and cross-frame sizes for use in the applicable jurisdiction and the details result in a relatively stiff brace that is suitable for most bridge geometries – particularly for bridges comprised of at least 4 girders across the width. However, multiple failures or problems of narrow girder units during construction provided insight into a buckling mode that was not addressed in design specifications. Figure 6a shows a twin girder system that is relatively common in bridge widenings or pedestrian bridges.

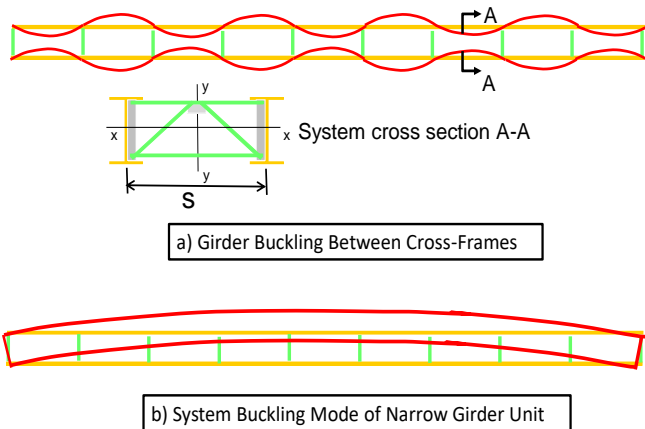


Figure 6: System Buckling Mode of Narrow Girder Units

The girder system may have closely-spaced cross-frames such as those indicated and the anticipated buckling mode of the compression flange along the length is one involving buckling between the cross-frame locations. However, an alternate mode that was recognized following a failure and other problematic bridge is the system mode depicted in Figure 6b in which the girder system buckles in a half-sine curve mode. The system mode is not sensitive to the spacing between the cross-frames and additional insight to the mode is provide in Section 3.2.

Yura et al. (2008) provided the elastic solution for the system mode that reflects both the St. Venant and warping terms similar to Eq. 1. However, the St. Venant term has a relatively low contribution and the following simplified expression provides good estimates of the critical buckling capacity:

$$M_{gs} = \frac{\pi^2 SE}{L_g^2} \sqrt{I_y I_x} \quad (17)$$

where, M_{gs} is the total system buckling resistance of the twin girder (ie. the buckling resistance per girder is half of M_{gs}), L_g is the span length of the girders, S is the center to center spacing of the adjacent girders, and I_x and I_y are the respective major and minor axis moments of inertia of a girder in the system. When Eq. 17 was being considered for incorporation into the 2015 interim AASHTO BDS, experiences (Sanchez and White 2012) with 2nd order amplification of a 3-girder mildly-curved bridge during construction raised concerns about using the full capacity from Eq. 17 for design. As a result, in the 2015 interim AASHTO BDS a limit of 50% of the capacity predicted by Eq. 17 was included. If the girder moments during construction exceeded this 50% limit, additional bracing or other changes were necessary. Subsequent work in Han and Helwig (2020) recommended raising the 50% limit to 70%, which is currently in AASHTO (2024). Han and Helwig also recommended applying a moment gradient factor, C_{bs} , specifically for the system buckling mode and recommended a value of 1.10 for simply-supported or partially-erected continuous girders and 2.0 for fully-erected continuous girder systems. Although Eq. 17 was originally derived for systems with doubly-symmetric girders, for singly-symmetric girders, I_y can be replaced with $I_{y\text{ eff}}$ as outlined in the discussion of Eq. 3. AASHTO (2024) also allows an effective section to be evaluated for non-prismatic girders using the method outlined by Reichenbach et al. (2020) in Section 3.1.2 of the present paper.

Equation 17 was specifically derived for twin girder systems; however, recommendations were made to approximate the behavior for systems with more than 2 girders. While studying the in-plane stiffness for torsional bracing applications, Fish et al. (2021, 2025) focused on the system buckling mode in the derivation. While the original focus was directed at torsional bracing systems, the actual stiffness of a system with any number of girders across the width (n_g) was determined leading to the following recommended modification to Eq. (17):

$$M_{gs} = C_{bs} \frac{\pi^2 SE}{L_g^2} \sqrt{I_y I_x \alpha_x} \quad (18)$$

$$\alpha_x = \frac{(n_g^2 - 1)}{12} \quad (19)$$

For girder systems with inadequate capacity, the system buckling capacity can be improved using a few panels of a top lateral truss near the ends of the span, which is included in AASHTO (2024). As an alternative to top flange lateral bracing, allowing a small length of concrete slab/deck to be placed near the ends of the section and allowed to cure a few days will also provide significant increases in the system buckling behavior since a condition near warping fixed will result.

3.2 Studies on Torsional Beam Bracing

While Section 3.1 was directed at solutions for evaluating the member or system buckling capacity, this section is directed at the means of improving stability with effective bracing. The studies

outlined in this section build off of the basic fundamentals that were discussed in Section 2.2. The focus is primarily directed at beam-torsional bracing and the improvements on the understanding of the basic behavior of these systems, and some of the changes that have resulted in design specifications as a result of this work.

3.2.1 Required Beam Torsional Brace Stiffness

The fundamentals of bracing were discussed earlier in Section 2.2. The pioneering work from Winter (1960) demonstrated that a stiffness higher than the ideal stiffness is necessary in order to control deformations and brace forces. The general philosophy on the many of the studies that have focused on various bracing systems is to provide a stiffness that limits the amount of deformation at the brace points to a value equal to the initial imperfection. Limiting the deformation to a value equal to the initial imperfection results in stability brace forces of $\beta \times \Delta_0$ or $\beta \times \theta_0$ depending on whether the lateral or torsional bracing systems are employed, respectively. For lateral bracing systems, the critical shape initial imperfection generally consists of a pure sweep, while torsional systems usually have a critical shape imperfection that consists of a lateral sweep of the compression flange while the tension flange remains straight (Wang and Helwig 2005). For lateral bracing systems (Winter 1960, Yura 2001) have demonstrated that providing a stiffness equal to twice the ideal stiffness results in good control of deformations such that the deformation is equal to the initial imperfection.

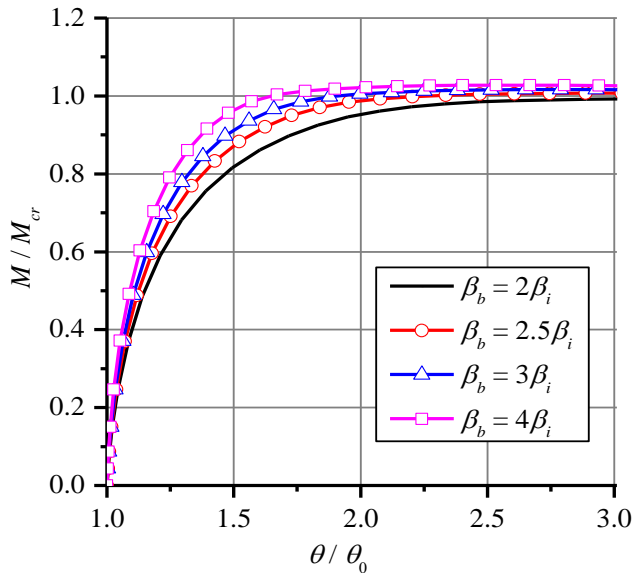


Figure 7: M/M_{cr} versus θ/θ_0 as a function of brace stiffness for torsional beam bracing.

Studies on torsional bracing systems for beams (Liu et al. 2020, Reichenbach et al. 2022) showed that a stiffness higher than twice the ideal stiffness was often necessary to limit the deformation to a value equal to the initial imperfection. Liu et al. 2020 considered the effects of load position, section geometry, and number of intermediate braces. Curves of the applied moment versus the twist as a function of the provided brace stiffness consistently took the form as shown in Figure 7. The moments are normalized by the critical moment corresponding to buckling between the brace points while the twist at the brace point was normalized by the magnitude of the initial imperfection. Following the conventional brace strength formulations, the target twist for $M/M_{cr} = 1$ was a value of θ/θ_0 of 2. The curves show that providing twice the ideal stiffness did not control the twist adequately. The studies by Liu showed that providing 3 x the ideal stiffness had much better control of the girder twist such that the strength requirements of $\beta \times \theta_0$ could be utilized in design. Therefore, in the AISC (2022) specification, the required torsional brace stiffness is a multiple of 3 times the ideal stiffness that was given in Eq. (3), leading to the following stiffness requirement:

$$\beta_{Ti} = \frac{3.6L}{nEI_{yeff}} \left(\frac{M_r}{C_b} \right)^2 \quad (20)$$

As torsional bracing provisions were being developed for the AASHTO (2022) specification, the value given in Eq. 20 was utilized for cases with a torsional brace depth less than 80% of the girder depth. However, when the brace depth is larger than 80% of the girder depth, a value of twice the ideal stiffness was specified, leading to a constant of 2.4 instead of 3.6 as shown in Eq. 20. The rationale for the lower stiffness was based upon the findings from Han and Helwig (2020) related to the system mode of buckling. In those studies, the likelihood of having the critical shape imperfection as specified in Wang and Helwig (2005) was investigated. As noted above, the critical shape was found to possess a lateral sweep of the compression flange with a straight tension flange. The magnitude of the compression flange lateral sweep was taken as a value of $L_b/500$, which is consistent with tolerances on the girder sweep. Although a beam may start with the critical shape imperfection, cross-frames and diaphragms are fabricated to fit into the girder system essentially assuming “perfect” girder geometry. Han and Helwig (2020) simulated cross-frame installation into a girder system with the critical shape geometry. Although the girders started with the critical shape geometry, the cross-frames tended to pull the compression flange closer to a straight position and pulled the tension flange more laterally, leading to an “imperfection” that was more of a pure sweep. The resulting brace forces in such a system are significantly reduced compared to a girder with the critical shape imperfection. Therefore, using twice the ideal stiffness was feasible when cross-frames are relatively deep compared to the girders being braced. With shallower braces (depth less than 80%), tolerances on bolt holes tend to impact the ability of the brace to “straighten” the girders. Therefore, the AASHTO bracing provisions recognize that in systems with more shallow braces such as through-girders where the torsional braces are the floor beams in the bridge, the required stiffness is as shown in Eq. (20); however, twice the ideal stiffness is required for systems with deeper braces.

3.2.2 Torsional Beam Bracing - In-Plane Girder Stiffness and Brace Stiffness

The stiffness behavior of bracing systems was discussed in Section 2.2. The three different stiffness components that impact torsional beam bracing were listed and the influence of the expression for springs in series given in Eq. 4 were outlined. The impact of the in-plane girder stiffness, β_g , was first recognized in the work documented in Helwig et al. (1993). To recognize the impact of the in-plane girders stiffness, a clear understanding of how torsional braces interact with the girder systems needs to be clear. Torsional braces generally refer to the restraint to beams

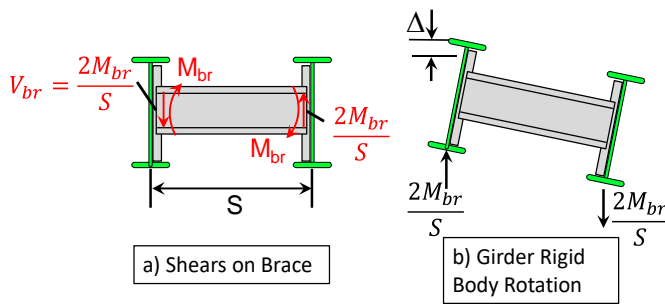


Figure 8: Brace shears lead to rigid body rotation of the girders that are a function of the in-plane stiffness.

provided by cross-frames or diaphragms such as those shown in Figure 8. Figure 8a shows that shears develop at the ends of the brace as a function of the girder spacing and restraining moments (torques on the girder). Equal and opposite shear develop on the girders leading to a rigid body rotation as depicted in Figure 8b. The magnitude of the rigid body rotation is a function of the in-plane stiffness of the girders and impact the overall stiffness of the torsional bracing system. Helwig et al.

(1993) considered the behavior of a midspan brace in a twin girder system and derived the following expression:

$$\beta_g = \frac{12S^2EI_x}{L^3} \quad (21)$$

Where, S is the girder spacing, I_x is the girder in-plane moment of inertia, and L is the girder span. Yura (2005) extended the in-plane stiffness derivation to a system with n_g girders across the width and replaced the “12” in equation 21 with the following expression:

$$N_g = \frac{24(n_g-1)^2}{n_g} \quad (22)$$

The expression from Yura yields 12 for twin girders but recognizes the reduced shear magnitudes and improved system stiffness for wider girder systems. For example, for a system with 5 girders across the width, Eq. 22 produces a constant of 77.

Although Eqs. 21 and 22 work well for twin girders with a midspan brace, the expressions can produce unconservative estimates for systems with more than one brace. In the development of Eqs. 21 and 22, it was thought that the critical case for the in-plane stiffness was a single brace at midspan since many bracing systems tend to undergo a succession in changes of mode shapes as the stiffness is increased until the girders finally buckle between the brace points. As a result, prior to the girders buckling between the brace points, if the girders were to buckle in one less “wave” in the buckled shape, some of the shears would be directed upwards and some downwards. However, most torsional bracing systems often stay in a half-sine curve buckled shape up until they finally buckle between the brace points when enough stiffness is reached in the bracing system. As a result – prior to buckling between the bracing points, all of the shears from the braces are in the same direction (up or down) and adding additional bracing lines makes the in-plane stiffness more critical.

Fish et al. (2021, 2025) focused on the use of the system buckling mode as discussed in Section 3.1.5 to develop an expression for the in-plane buckling behavior. Such an approach is warranted since the system mode of buckling is closely linked to the in-plane stiffness. As noted earlier, the capacity in the system mode of buckling is relatively unaffected by the spacing between the braces. Phrased another way, when the system mode of buckling controls the girder capacity – decreasing the spacing or increasing the cross-frame stiffness will not improve the behavior. From a bracing perspective, because torsional bracing systems are controlled by the expression for springs in series given in Eq. 4, when in the in-plane stiffness component β_g is less than the required torsional stiffness (ie. Eq. 20), increasing the stiffness of the brace will not result in adequate bracing – even if an infinitely stiff brace is used. Instead, the system will buckle in the half-sine “system” mode.

The derived equation from the system mode of buckling recommended in Fish et al. (2025) consists of the following expression:

$$\beta_{g,2025} = \frac{\pi^4 EI_x S^2 \alpha_x}{L^3 (n + 1)} \quad (23)$$

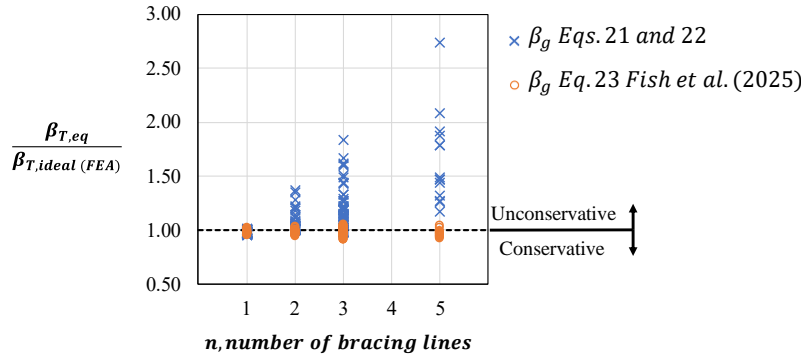


Figure 9: Comparison of In-plane Stiffness Components, β_g .

element models. Establishing the ideal stiffness requirements requires multiple models with various geometries as outlined in Fish et al. (2025). The equations from Helwig et al. (1993) and Yura (2001) that were based upon a system with a single brace line at midspan work well for that specific case ($n=1$); however, become unconservative for girders with more bracing lines. Equation 23 developed by Fish et al. (2025) has good agreement with the eigenvalue buckling expressions from 3D finite element models. Based upon the improved accuracy of Eq. 23, ballots will likely be put forth for consideration for the 11th edition of AASHTO.

3.2.3 Studies on the Torsional Brace Stiffness

With regard the three components for torsional bracing system that were outlined earlier, the stiffness that should be best understood is that of the brace itself. However, over the past 10 years studies have shown that the understanding of the brace stiffness is not as clear as believed – particularly for cross-frame systems. Cross-frames are truss-type elements that most often consist of X-frames (two active diagonals), K-frames, or Z-frames (single diagonal and two struts). Yura (2001) derived stiffness expressions for all three geometries and are essentially exact for the specific assumptions they were derived with the following expressions:

$$\beta_{br-z} = \frac{ES^2h_b^2}{\frac{2L_c^3}{A_c} + \frac{S^3}{A_h}} \quad (24)$$

$$\beta_{br-x} = \frac{A_c ES^2 h_b^2}{L_c^3} \quad (25)$$

$$\beta_{br-z} = \frac{ES^2h_b^2}{\frac{8L_c^3}{A_c} + \frac{S^3}{A_h}} \quad (26)$$

Where, h_b is the depth of the cross-frame, S is the girder spacing, L_c is the length of the diagonal member, A_c is the area of the diagonal member, and A_h is the area of the horizontal strut members. Recent studies have focused on the behavior of fabricated cross-frames as well as the stiffness of cross-frame systems.

Where, α_x is defined in Eq. 19, and n is the number of intermediate bracing lines along the span length. A comparison between the β_g predictions using the expressions from Eqs. 21 and 22 versus the values predicted from Eq. 23 are shown in Figure 9. The expressions have been normalized by predictions of the ideal stiffness required from eigenvalue buckling analyses with three-dimensional finite

Much of the finite element analysis that was carried out on the systems was conducted by Dr. Aidan Bjelland – and was extremely important with regards to confirming the accuracy of the Fish (2021) derivations. One of the difficult aspects of the work on in-plane stiffness documented in Fish et al. (2025) was isolating the various stiffness components – and establishing an accurate value of the ideal brace stiffness. To validate the in-plane stiffness expressions, the stiffness of the brace needed to be accurately determined. Because the in-plane stiffness is a function of the girder spacing – the in-plane stiffness could effectively be made infinite by using a large girder spacing. Because full depth cross-frames were utilized, the effects of cross-section distortion were also eliminated leaving only the brace stiffness. The original derivations from Yura (2001) were based upon a twin girder connected by a single cross-frame.

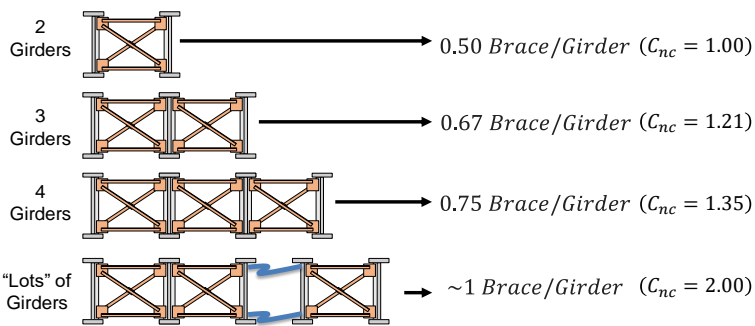


Figure 10: Improved efficiency with added braces demonstrating “ C_{nc} term”.

However, when additional girders are added, the effective number of braces per girder increases as depicted in Figure 10. With a single cross-frame between two girders, there is effectively 0.5 braces per girder. As additional girders are added, the effective number of braces approach 1 brace per girder. From a stiffness perspective, Yura’s equations were derived as the stiffness per cross-frame – which assumes 0.5

cross-frames per girder. Therefore, the effective brace stiffness ($\beta_{br,eff}$) can be evaluated using the following expression:

$$\beta_{br,eff} = C_{nc}\beta_{br} \quad (27)$$

Where, β_{br} is the stiffness from Equations (24) – (26) for the appropriate cross-frame geometry and C_{nc} is the stiffness modifier that accounts for the number of braces relative to the number of girders, n_g . The expressions derived based upon curve fits with FEA studies are given in the following equations for X, K, and Z systems:

$$C_{nc,X,K} = 1 + \frac{n_g - 2}{n_g + 1.75} \quad (28)$$

$$C_{nc,Z} = 1 + \frac{n_g - 2}{n_g + 0.75} \quad (29)$$

Equation 28 was compared with FEA solutions that demonstrate the improved efficiency and accuracy of the equation in Figure 11 for an X-system; however similar agreement was achieved with K and Z systems. The graph shows the required brace stiffness to achieve buckling between the brace points (ideal stiffness) as a function of the number of girders across the width of the system. Four different girder sections to vary geometrical proportions were used and the geometries can be found in Fish et al. (2025). The vertical axis was normalized by the ideal stiffness for twin girder (ie. one brace between the girders). For the specific case of 2 girders, Equation 25 from Yura (2001) for an X-system is essentially exact. When more than 2 girders are

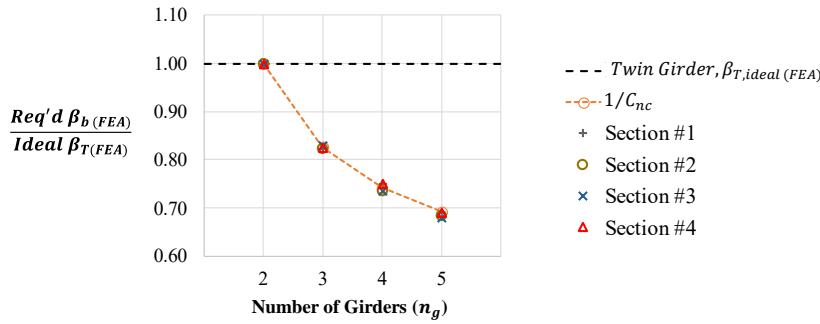


Figure 11: Torsional brace stiffness efficiency increases with more girders.

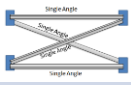
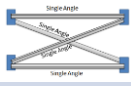
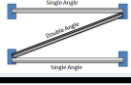
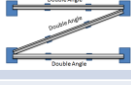
differences between the analytical brace stiffness equations (Eqs. 24-26) versus as-fabricated cross-frames was documented in Battistini et al. (2013, 2016) that summarized the findings from an experimental and FEA parametric study. The full experimental and FEA studies are documented in Wang (2013). The experiments consisted of stiffness and strength tests on cross-frames with various member configurations. Cross-frames are usually comprised of single-angle members or WT sections that often lead to eccentric connections. The investigation was also considering single-diagonal members that made use of concentrically-loaded members. Table 1 summarizes the stiffness measurements along with comparisons between the analytical solutions (Eqs. 24-26) and FEA predictions.

A comparison between the laboratory experiments and the analytical solution show that cross-frames with concentric connections agree almost exactly with the predictions from the Yura (2001) equations; however, cross-frames with eccentric connections (single-angle members) lead to very significant unconservative estimates. The truss model idealization assumes all of the deformation in the cross-frame members are due to axial shortening; however, the eccentric connection leads to member bending as well – which softens the cross-frame. Although the shell element models can accurately predict the stiffness of the systems with eccentric connections, such models are impractical for design. Therefore, recommendations were made to utilize the analytical expressions (or line element models in computer programs – which agree exactly with Yura’s equations) and to apply a reduction factor to account for the reduction in stiffness from the eccentric connections. Since 2015, the AASHTO BDS Chapter 4 has recommended reducing the stiffness of the cross-frames by 35 percent by modifying the member area by a factor of 0.65 when evaluating the performance of cross-frames in straight and curved girder bridges during construction. Reichenbach et al. (2022) and Park et al. (2023) studied the behavior in cross-frames in fatigue (composite girders) and recommended a reduction factor of 25 percent by modifying the member area by a factor of 0.75. These recommendations were balloted and included in the 10th Edition of AASHTO (2024) for both the stability bracing provisions and cross-frame fatigue provisions.

used, the required cross-frame stiffness to achieve buckling between the brace points is reduced relative to the case with 2 girders. A graph of the inverse of Equation (28) matches the FEA predictions very accurately. Based upon the improved accuracy using the C_{nc} modifiers, a ballot will likely be developed for consideration for the 11th edition of AASHTO.

Another study that recognized

Table 1: Comparisons between Experiments, Analytical Solutions, and FEA Predictions for Cross-Frame Stiffness

Type of Cross Frames		Test Results	Analytic Solution	Error %	Line Element Solution	Error %	Shell Element Solution	Error %	
Eccentric Connections	Single Angle X Frame		872,000	1,579,000	82%	1,572,000	81%	867,000	-1%
	Single Angle K Frame		760,000	1,189,000	56%	1,180,000	55%	781,000	3%
	Unequal Leg Angle X Frame		1,054,000	1,609,000	53%	1,614,000	53%	1,065,000	1%
	Double Angle Z (Single Struts)		597,000	907,000	52%	905,000	52%	616,000	3%
	Double Angle Z (Double Struts)		1,182,000	1,152,000	-2.5%	1,152,000	-2.5%	1,164,000	-1.5%
	Square Tube Z-frame		658,000	649,000	-1%	647,000	-2%	657,000	0%

3.2.4 Cross-frame Lean-on Bracing Systems

A great deal of work has been underway since the late 1990's that is focused on improving the efficiency of cross-frame systems and minimizing truck-induced stresses that adversely impact the fatigue resistance of cross-frames. Because single-angle members have the worst fatigue rating of E' , minimizing the truck-induced stress range is very important. Lean-on bracing concepts were developed for steel bridges with recommendations originally summarized and published in Wang (2002), Helwig and Wang (2003), and Romage (2008). The concepts involve selectively eliminating full cross-frames in a given bracing line and instead providing top and bottom struts

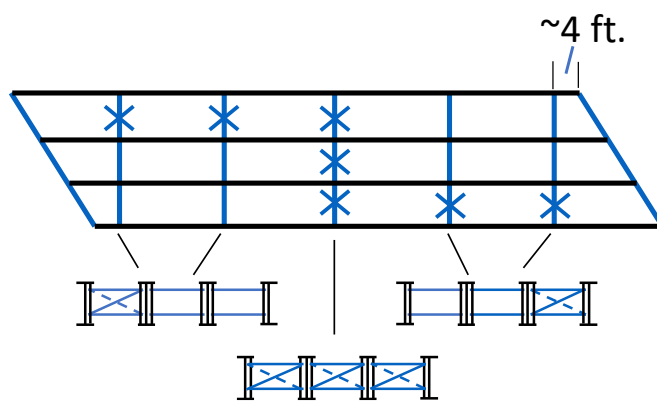


Figure 12: Lean-on Cross-Frame Bracing Concepts

to provide a load path to lean several girders on a single cross-frame as depicted in Figure 12. Cross-frame lines that frame into a support section should be offset from the support by 4~5 ft. to avoid large live load induced stresses that adversely impact fatigue performance. In addition, the support regions are often congested regions and moving the bracing line away from the support reduces this congestion. As depicted in the plan view of the 4-girder system, in a given line, cross-frames should be moved as far from the support as possible to achieve the best live load performance as far as truck induced stresses. The National Steel Bridge

Alliance recently published a design guide that was developed based upon the previous lean-on bracing work (Holt et al. 2022).



Figure 13: Lean on Cross-Frame Bracing in Heavily Skewed Bridge.



Figure 14: Bent Plate Details Used on Heavily Skewed Bridge

Improved and enhanced lean-on bracing provisions were also developed in a recent study sponsored by the Texas Department of Transportation (TxDOT Project 0-7093 - Bjelland et al. 2025). The work builds off the previous work summarized in Wang (2002) and Helwig and Wang (2003) and provides significant enhancements on all aspects of lean-on bracing applications. There have been a number of bridges built using lean-on bracing, one of which is shown in Figure 13. In many cases, the number of intermediate cross-frames can be substantially reduced leading to improved efficiency as well as better resistance to fatigue problems. As discussed in Section 3.1.4, in bridges with heavily skewed supports such as in Figure 13, improved performance can be achieved utilizing the half-round bearing stiffeners at the support regions where cross frames are parallel to the skew. Figure 14 shows the significant eccentricity and flexibility that the commonly-used bent plates cause. These details do not have the ability to engage the full stiffness of the cross-frame.

4. Summary

This paper focused on a number of studies conducted over the past 30 years related to girder stability and bracing. The studies targeted a number of common issues that arise in practical design problems. While many design solutions focus on problems with prismatic sections or well-defined bracing, during erection and other stages of construction, the bracing varies significantly and in some cases, such as lifting girders with a crane – is totally absent. The longer unbraced lengths of the girders often result in non-prismatic sections and solutions were presented to address these issues. In addition to conventional LTB, the limit state of system buckling for narrow girder units that was discovered around 2005 was discussed along with simple buckling expressions that were developed. Stability problems such as the system buckling mode are closely tied to some of the factors that impact stability bracing – such as the impact of the in-plane stiffness on cross-frame or diaphragm behavior. A number of recent studies have resulted in significant improvements in the understanding of torsional bracing systems. Improved design solutions have been developed for many factors for torsional bracing that recognize the stiffness components of both the brace and the in-plane girder stiffness. Many of these past studies have resulted in solutions that have been incorporated into the AISC Specifications for Buildings as well as the AASHTO Bridge

Design Specifications. Some of the more recent work has not been considered for inclusion into the specifications; however, may be considered in the future.

Acknowledgments

Throughout my career, numerous designers, erectors, and fabricators have brought my attention to a number of problems that did not have viable solutions that have helped steer my career in a fun direction. Many of these individuals were representatives of committees within the SSRC Task Groups, the AISC Specification Task Committees, the National Steel Bridge Alliance, and the AASHTO Steel Bridge Task Force – while others were engineers that asked great questions during continuing education presentations. I want to acknowledge all these past individuals for helping to steer my career in the right direction towards interesting problems. As a faculty supervisor – we often get much of the credit for the solutions that get developed; however, I'd like to acknowledge all of the intelligent and hard-working students I have had the pleasure of working with on the studies outlined in this paper – as well as many of the interesting studies that I was not able to include due to space limitations. The success of any research study is always rooted in the individuals that lead the experiments or carry out the parametric FEA studies. I also had a number of colleagues that were involved with these research studies that contributed significantly to direction and the success of the studies. I have been blessed throughout my career to work with so many talented individuals and I thank you all for the companionship while working towards solutions and more importantly the friendships that have developed. Finally, I have been fortunate to come from a state where the Department of Transportation recognizes the benefits of research and I am very grateful for the funding I have received throughout my career from TxDOT.

References

- AASHTO (American Association of State Highway and Transportation Officials). (2024). LRFID Bridge Design Specifications 10th Edition. Washington, DC: AASHTO.
- AISC (American Institute of Steel Construction). (2022). Specification for Structural Steel Buildings. Chicago, IL: AISC.
- Battistini, A., Wang, W., Donahue, S., Helwig, T., Engelhardt, M., and Frank, K. (2013) “Improved Cross Frame Details,” Research Report 0-6564.
- Battistini, A., Wang, W., Helwig, T., Engelhardt, M., and Frank, K. (2016). “Stiffness behavior of cross frames in steel bridge systems.” *J. Bridge Eng.* 21 (6): 04016024. [https://doi.org/10.1061/\(ASCE\)BE.1943-5592.0000883](https://doi.org/10.1061/(ASCE)BE.1943-5592.0000883).
- Liang, C., Xiong, Z., Helwig, T., Reichenbach, M., and Pan, Z. (2024) “Effects of Shear on The Elastic Lateral Torsional Buckling of Singly-Symmetric I-Beams,” <https://doi.org/10.1016/j.tws.2024.112174>, *Thin-Walled Structures, Elsevier*, Vol. 203.
- Farris, J. (2008). “Behavior of Horizontally Curved Steel I-Girders During Construction.” (2008) Master’s thesis, Dept. of Civil, Architectural, and Environmental Engineering, Univ. of Texas at Austin, Dec 2008.
- Fish, D. (2021) “Refined Design Expressions for In-Plane Girder Stiffness and System Buckling Capacity.” (2021) Master’s thesis, Dept. of Civil, Architectural, and Environmental Engineering, Univ. of Texas at Austin, Dec 2021.
- Fish, D., Bjelland, A., Park, Sunghyun, Helwig, T., and Engelhardt, M., (2025). “Improved Design Expressions for the Global Buckling Capacity and In-Plane Girder Stiffness of Torsional-Braced I-Girder Systems, Accepted for publication in *ASCE Journal of Structural Engineering*.
- Galambos, T. V. (1968). *Structural members and frames*, Prentice Hall, Englewood Cliffs, NJ.
- Han, L. and Helwig, T. (2020). “Elastic Global Lateral-Torsional Buckling of Straight I-Shaped Girder Systems.” *ASCE J. Struct. Eng.* 146 (4): 04020043. [http://dx.doi.org/10.1061/\(ASCE\)ST.1943-541X.0002586](http://dx.doi.org/10.1061/(ASCE)ST.1943-541X.0002586).
- Helwig, T., Frank, K., and Yura, J. (1993). “Bracing forces in diaphragms and cross frames.” In *Proc., Structural Stability Research Council Conf.*, 6–7. Milwaukee, WI: Structural Stability Research Council.
- Helwig, T. A., Frank, K. H., and Yura, J. A. (1997). “Lateral-torsional buckling of singly symmetric i-beams.” *J. Struct. Eng.*, 123(9) 1172-1179.
- Holt, J.M., Romage-Chambers, M., Chad, C., Panchal, D., and Wasserman, E. (2022) “Lean-on Bracing Reference

- Guide”, National Steel Bridge Alliance - *AISC*.
- Liang C, Reichenbach MC, Helwig TA, Engelhardt MD, Yura JA. (2022) Effects of Shear on the Elastic Lateral Torsional Buckling of Doubly Symmetric I-Beams. *J Struct Eng.* 148:04021301. [https://doi.org/10.1061/\(ASCE\)ST.1943-541X.0003294](https://doi.org/10.1061/(ASCE)ST.1943-541X.0003294).
- Liu, Y. Kövesdi, B., and Helwig, T. (2020). “Strength and stiffness requirements for beam torsional bracing.” In *Proc., Structural Stability Research Council Conf.*, Atlanta, GA: Structural Stability Research Council.
- Ojalvo, M., and Chambers, R. S. (1977). “Effects of warping restraints on I-beam buckling.” *J. Struct. Div.*, 103(12), 2351–2360.
- Park, S., Reichenbach, M., Helwig, T., Engelhardt, M., Connor, R., and Grubb, M. (2023). “Improved Cross-Frame Analysis and Design: Wide-Flange T-Shape Sections.” Final Report NCHRP 12-113. <https://doi.org/10.17226/27087>.
- Quadrato, C., Engelhardt, M., Battistini, A., Wang W., Helwig, T.A., and Frank, K. (2010) “Cross-Frame and Diaphragm Layout and Connection Details,” Research Report 0-5701.
- Quadrato, C., Battistini, A., Helwig, T., Engelhardt, M., and Frank, K. (2014) “Increasing Girder Elastic Buckling Strength using Split Pipe Bearing Stiffeners,” *ASCE Journal of Bridge Engineering*, Vol. 19, No. 4, [https://doi.org/10.1061/\(ASCE\)BE.1943-5592.0000550](https://doi.org/10.1061/(ASCE)BE.1943-5592.0000550).
- Reichenbach, M., Liu, Y., Helwig, T., Engelhardt, M. (2020). “Lateral-Torsional Buckling of Singly Symmetric I-Girders with Stepped Flanges.” *ASCE J. Struct. Eng.* 146 (10): [https://doi.org/10.1061/\(ASCE\)ST.1943-541X.0002780](https://doi.org/10.1061/(ASCE)ST.1943-541X.0002780).
- Reichenbach, M., White, J., Park, S., Zecchin, E., Moore, M., Liu, M., Liang, C., Kövesdi, B., Helwig, T., Engelhardt, M., Connor, R., and Grubb, M. (2021). “Proposed Modification to AASHTO Cross-Frame Analysis and Design.” National Cooperative Highway Research Program, Transportation Research Board, National Academies of Sciences, Engineering, and Medicine, Transportation Research Board. <https://doi.org/10.17226/26074>.
- Romage, M. (2008). “Field Measurements of Lean-on Bracing for Steel Girder Bridges with Skewed Supports” Master’s thesis, Dept. of Civil, Architectural, and Environmental Engineering, Univ. of Texas at Austin, Dec 2008.
- Sanchez, T.A., White, D.W. (2012). “Stability of curved steel I-girder bridges during construction”. *Transportation Research Record: Journal of the Transportation Research Board*, 2268, 122-129.
- Schue, A. (2008). “Behavior of Horizontally Curved Steel I-Girders During Lifting.” Master’s thesis, Dept. of Civil, Architectural, and Environmental Engineering, Univ. of Texas at Austin, May 2008.
- Stith, J., Schuh, A., Farris, J., Petrucci, B., Helwig, T., Williamson, E., Frank, K., Engelhardt, M., and Kim, H-J., (2010) “Guidance for Erection and Construction of Curved I-girder Bridges,” Research Report 5574-1, May 2010.
- SSRC (2010). *Stability design criteria for metal structures, 6th Ed.*, Structural Stability Research Council, New York Edited by R. Ziemian.
- Taylor, A., and Ojalvo, M. (1966). “Torsional Restraint of Lateral Buckling.” *J. Struct. Div.* 92 (ST2), 115-129. <https://doi.org/10.1061/JSDEAG.0001414>.
- Timoshenko, S., and Gere, J. (1961). *Theory of Elastic Stability*. McGraw-Hill, New York.
- Wang, L. (2002). “Cross-frame and Diaphragm Behavior for Steel Bridges with Skewed Supports.” Ph.D. dissertation, Univ. of Houston, Houston, Texas.
- Wang, L. and Helwig, T. (2005). “Critical Imperfections for Beam Bracing Systems”. *J. Struct. Eng.*, pp. 933-940 [https://doi.org/10.1061/\(ASCE\)0733-9445\(2005\)131:6\(933\)](https://doi.org/10.1061/(ASCE)0733-9445(2005)131:6(933)).
- Wang, W. (2013) “A Study of Stiffness of Steel Bridge Cross Frames”. PhD Dissertation, Dept. of Civil, Architectural, and Environmental Engineering, Univ. of Texas at Austin, Aug. 2013.
- Winter G. (1943). Lateral Stability of Unsymmetrical I-Beams and Trusses in Bending. *Trans Am Soc Civ Eng* 1943; <https://doi.org/10.1061/TACEAT.0005677>.
- Winter, G. (1960). “Lateral Bracing of Columns and Beams.” *Transactions of the ASCE*. 125 (1): 809–825. <https://doi.org/10.1061/TACEAT.0007917>.
- Yura, J. (2001). “Fundamentals of Beam Bracing.” *Engineering Journal*, 38 (1), 11–26. <https://doi.org/10.62913/engj.v38i1.750>.
- Yura, J., Helwig, T., Herman, R., and Zhou, C. (2008). “Global Lateral Buckling of I-Shaped Girder Systems.” *ASCE J. Struct. Eng.* 134 (9): 1487-1494. [https://doi.org/10.1061/\(ASCE\)0733-9445\(2008\)134:9\(1487\)](https://doi.org/10.1061/(ASCE)0733-9445(2008)134:9(1487)).